

Autonomous Downlink Power Control for LTE Femtocells based on Channel Quality Indicator

Xiang Xu, Gledi Kutrolli and Rudolf Mathar

Institute for Theoretical Information Technology, RWTH Aachen University
Aachen, Germany 52074

Email: {xu,kutrolli,mathar}@ti.rwth-aachen.de

Abstract—In this work, a downlink power control scheme based on channel quality indicator (CQI) is proposed for LTE femtocells. Unlike the conventional methods, this scheme takes the service types of users into account. Without making strong assumptions, such as full knowledge of the network or perfect coordination among basestations, a completely decentralized solution is provided. Simulation results confirm, that comparing to the conventional schemes, better throughput and coverage can be achieved simultaneously by the proposed algorithm.

Index Terms—Femtocell, power control, LTE, CQI

I. INTRODUCTION

Long-Term Evolution (LTE) is aiming at providing ubiquitous connectivity. However, indoor users usually suffer from strong penetration loss due to the building walls. Therefore, femtocells are proposed as an economical solution to serve indoor user equipments (UE) [1]. Femtocells introduce Home evolved Node B (HeNB) as low-power short range base stations, which are connected to the backhaul network via broadband. With the isolation provided by the building walls, HeNB can fill the indoor coverage hole with efficient spatial reuse of the spectrum [2] [3].

The deployment of femtocells can be categorized in different ways. According to access mode, they can be divided into open access and closed subscriber group (CSG), while open access grant every user the right to connect to a femtocell, and CSG gives service only to the users with proper licences [4]. According to spectrum usage, femtocells can either share the same frequency band as the macrocell or use a dedicated frequency band [5].

Whenever a channel is shared between the femtocell and macrocell, co-channel interference (CCI) is inevitable. Especially for CSG, macrocell UE (MUE) close to a femtocell could be severely interfered, if the HeNB is serving the home UE (HUE) with maximal transmit (Tx) power. Therefore, the necessity of interference mitigation must be addressed [6]. Interference mitigation can be achieved in different ways, such as radio resource management, handover optimization and HeNB power control, which will be elaborated in this paper.

Nowadays, since data communications occupies the majority of bandwidth, cellular networks show an asymmetric

behavior, that is, the downlink data rate is much higher than the uplink data rate. Therefore, in this paper, only downlink power control is considered. Furthermore, this paper is not aiming at the theoretical optimal solution, but devoted to finding an effective and practical heuristic, which could be easily implemented in the real system.

In previous works, an adaptive power control based on signal to interference ratio (SIR) at cell edge is described in [4], where full knowledge of network layout is required in this approach. A distance based method is proposed in [7], which guaranties that the HUE has at least the same receive power as an MUE in the same location but without building walls. This model also requires a large amount of information, such as cell locations, power levels, antenna orientations and gains etc.. In addition this model relies heavily on a reliable pathloss model. Another scheme based on the measured received power from eNB is also proposed in [7], where no location information is required. In [8], another adaptive power control scheme is proposed to utilized not only the downlink Rx power from macrocell but also the uplink Rx power from MUE. These methods aim at providing the same quality of service (QoS) for the HUE as they are outdoor UEs served by macrocell. As a drawback, for the area on cell edges, where the macrocell signal level is already poor, femtocells are not able to deliver good performance for HUEs. Furthermore, the data rate requirement of different service types are not taken into consideration. The result is, the Tx power is more than enough for some service which requires only a small data rate.

In this work, an autonomous power control scheme based on CQI feedback is proposed. CQI, as specified in 3GPP, is a four-bit value sent from UE to eNB or HeNB [9]. CQI indicates the level of signal to interference plus noise ratio (SINR) of a certain frequency band in downlink channels. Each CQI level corresponds to a specific modulation and coding scheme (MCS). Based on CQI feedback, the adaptive modulation and coding (AMC) is engaged, where different levels of data rate and error protection can be provided. Thus, CQI does not only show the channel condition, but also implies QoS. The proposed scheme works in self-organizing manner by utilizing the CQI feedback. When compared with some of the aforementioned schemes, the proposed scheme shows superior performance in throughput and coverage in simulations.

This research was partly supported by the UMIC excellence cluster of RWTH Aachen University.

II. PRELIMINARIES

The co-deployment of macro and femtocell makes a heterogeneous network, where UEs can be served by either eNBs or HeNBs through radio links. As shown in Fig. 1 (a), the building wall produces a penetration loss of 10-20 dB, which provide good suppression of inter-cell interference (ICI).

Consider a partial sharing channel, in which the spectrum of HeNB is a subset of whole spectrum for eNB. The shared subset can be reused by both macro and femtocell, as shown in Fig. 1 (b).

Since the femtocells are meant to be deployed by the end user to boost their indoor signal coverage, CSG is much more likely to be the access mode, where the licensed UE can be served by femtocells but the unlicensed UE close to a HeNB would have interference from the femtocell.

Furthermore, in this work, realistic restrictions from LTE are applied, namely, although both eNB and HeNB are connected to the backhaul network with wired broadband connections, the communication between eNB and HeNB is only at coarse time scale. That means, HeNB can not be controlled by eNB in a realtime centralized fashion. Therefore, a decentralized solution is preferred.

A. System model

Assuming a HUE receives signal from F femtocells, in a cellular network with M eNBs, the SINR of the HUE u served by HeNB f can be written as

$$\gamma_u = \frac{P_{f,u}^{(FC)}}{\sum_{i=1}^M P_{i,u}^{(MC)} + \sum_{j=1, j \neq f}^F P_{j,u}^{(FC)} + N_u}, \quad (1)$$

where $P_{f,u}^{(FC)}$ is the Rx power from femtocell, $P_{i,u}^{(MC)}$ is the Rx power from the i th macrocell, $P_{j,u}^{(FC)}$ is the Rx power from the j th femtocell and N is the thermal noise power.

Similarly, the SINR of a MUE v served by eNB m can be written as

$$\gamma_v = \frac{P_{m,v}^{(MC)}}{\sum_{i=1, i \neq m}^M P_{i,v}^{(MC)} + \sum_{j=1}^F P_{j,v}^{(FC)} + N_v}, \quad (2)$$

where the interference from femtocell $P_{j,v}^{(FC)}$ exists, if the MUE is close enough to a femtocell.

The macrocell Rx power $P_{i,u}^{(MC)}$ is calculated by

$$P_{i,u}^{(MC)} = \frac{P_{Tx,i}^{(MC)} G_{Tx,i}^{(MC)} H_{i,u}^{(MC)}}{L_{i,u}^{(MC)}} \quad (3)$$

where $P_{Tx,i}^{(MC)}$, $G_{Tx,i}^{(MC)}$ are the Tx power and antenna gain of the i th eNB, $H_{i,u}^{(MC)}$ and $L_{i,u}^{(MC)}$ are the normalized channel gain and pathloss of the wireless link between the i th eNB and u th UE, respectively. The Rx power of femtocell $P_{f,u}^{(FC)}$ can be calculated in the same way.

Due to multipath propagation and movements of UE, the wireless channel for broadband communications shows a

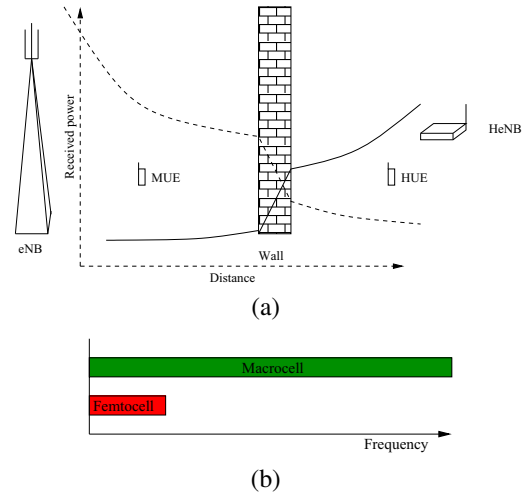


Fig. 1. (a) Heterogeneous network deployment. (b) Partial frequency sharing.

doubly selective property, namely, the channel gain $H_{i,u}^{(MC)}$ varies both on frequency and time domain [10]. The frequency domain variations, which depend on the propagation environment, are commonly described by the power-delay profile (PDP). And time domain variations, which relate to movements, are normally characterized by the Rayleigh fading model [11]. It is assumed that the channel gain is static in one physical resource block (PRB), which is the basic unit of resource allocation. One PRB contains 12 consecutive subcarriers in frequency domain and 0.5 ms in time domain.

The SINR can be measured by the UE and sent back to eNB or HeNB in the form of CQI. To reduce the signaling overhead, the generation of CQI consists two steps of compression. Firstly, the SINR of a group of PRBs (called subband), is mapped in to an effective signal to noise ratio (SNR), as shown in Fig. 2 (a) [12]. And secondly, according to the 3GPP LTE standards, the effective SNR is mapped into a 4-bit message, representing 16 levels of CQI through a linear step function, as shown in Fig. 2 (b). When the basestation transmits with the corresponding MCS of CQI, a block error rate (BLER) smaller than 10% can be guaranteed. For the sake of simplicity, in this work, the CQI feed back is assumed to be on PRB level, and the SINR is directly mapped into CQI.

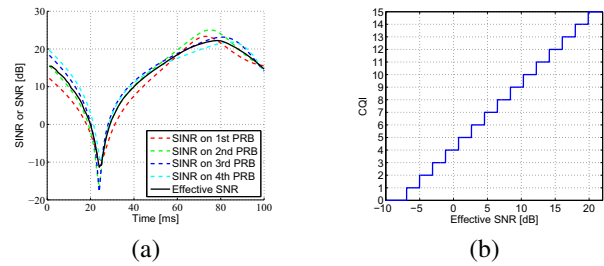


Fig. 2. (a) SINR to effective SNR mapping for a subband consisting 4 PRBs. (b) SNR to CQI mapping.

B. Traffic model

Since different services have different requirement on data rate and Tx power, specific traffic models must be taken into account.

Generally, the data traffics can be classified into two groups according to QoS requirements. One is the margin adaptive (MA), for which the Tx power should be minimized, while satisfying data rate requirements. The other one is rate adaptive (RA), for which the data rate should be maximized subject to the power limit[13].

According the services, three kinds of UEs are considered in this work, the information about the UE classification are summarized in Tab. I, where the data rate requirement of data user is a fixed value ranging from 512 kbps to 2000 kbps.

Service	Priority	Data rate	Type	Percentage
VoIP	High	64 kbps	MA	10%
Data	Mid	[512-2000] kbps	MA	40%
Web	Low	≥ 64 kbps	RA	50%

TABLE I
DIFFERENT TYPES OF UE

C. Resource allocation

Since no real-time information exchange between eNBs and HeNBs is assumed, the resource allocation works in a decentralized manner. The HeNB first sorts its HUEs according to their priority. The HUE with the highest priority picks its PRBs with higher CQI until the data rate requirement is fulfilled. This procedure goes on successively, until each HUE meet its data rate requirement. After that, the rest of the PRBs are equally assigned to the RA users. The resource allocation in the macrocell is performed in the same way, regardless the assignment of femtocells.

III. AUTONOMOUS POWER CONTROL

In this work, the novel CQI-based power control scheme is compared with two different existing schemes, namely, the distance-based power control and the measurement-based power control [7].

A. Distance-based power control

The femtocell Tx power $P_{\text{Tx,dist}}^{(\text{FC})}$ is configured such that the UE at a defined radius r would receive at least the same amount of power from the strongest macrocell with building walls. The HeNB Tx power can be calculated as

$$P_{\text{Tx,dist}}^{(\text{FC})} \triangleq \min\left(\frac{P_{\text{Tx,m}}^{(\text{MC})} G_{\text{Tx,m}}^{(\text{MC})} L_f^{(\text{FC})}(r)}{L_{m,f}^{(\text{MC})}}, P_{\text{Tx,max}}^{(\text{FC})}\right), \quad (4)$$

where $P_{\text{Tx,max}}^{(\text{FC})}$ is the maximum Tx power of HeNB. $L_{m,f}^{(\text{MC})}$ is the pathloss between eNB and HeNB including the wall penetration loss, and $L_f^{(\text{FC})}(r)$ is the estimated pathloss from the femtocell to a UE at the target femtocell radius r . Effectively,

the estimated Rx power of macrocell m at the location of the HeNB:

$$\hat{P}_{m,f}^{(\text{MC})} = \frac{P_{\text{Tx,m}}^{(\text{MC})} G_{\text{Tx,m}}^{(\text{MC})}}{L_{m,f}^{(\text{MC})}} \quad (5)$$

is used to determine the Tx power of HeNB. However, since $L_{m,f}^{(\text{MC})}$ and $L_f^{(\text{FC})}(r)$ are calculated by using empirical pathloss models, they are highly unreliable.

B. Measurement-based power control

The measurement-based model takes one step further. The estimated Rx power at HeNB location is replaced by the measured Rx power, supposing the HeNB has the function of doing this measurement. And the Tx power of HeNB becomes

$$P_{\text{Tx,meas}}^{(\text{FC})} \triangleq \min(P_{m,f}^{(\text{MC})} L_f^{(\text{FC})}(r), P_{\text{Tx,max}}^{(\text{FC})}), \quad (6)$$

where $P_{m,f}^{(\text{MC})}$ is the measured Rx power at the location of HeNB.

C. CQI-based power control

In the proposed CQI-based power control, UEs with different types of service are treated differently. Being initialized with the minimum Tx power $P_{\text{Tx,min}}^{(\text{FC})}$, HeNBs increase their Tx power, while assessing the CQI feedback Q of HUEs. For HeNBs serving only VoIP users and data users, as soon as the data rate requirement can be met, the increase stops. For web users, an additional offset throughput α is set upon the minimum data rate requirement. The serving HeNB stops increasing the Tx power when the additional throughput is achieved. Therefore, the web users can at least get an incremental throughput of α . The algorithm is described in Alg. 1, where R is the required CQI for the UE to achieve the target data rate, $N_{\text{PRB},u}^{(\text{FC})}$ is the number of PRBs for HUE u , $N_{\text{PRB}}^{(\text{FC})}$ is the total number of PRBs for femtocells, $T_{\text{min},u}^{(\text{FC})}$ is the minimum data rate requirement for web UE and $T_{\text{target},u}^{(\text{FC})}$ is the target data rate for UE u , $T_{\text{target}}^{(\text{FC})}$ is the target throughput for

Algorithm 1 Power control algorithm based on CQI

```

for each HeNB do
   $P_{\text{Tx,CQI}}^{(\text{FC})} = P_{\text{Tx,min}}^{(\text{FC})}$ 
  for each web UE do
     $T_{\text{target},u}^{(\text{FC})} = T_{\text{min},u}^{(\text{FC})} + \alpha$ 
  end for
   $T_{\text{target}}^{(\text{FC})} = \sum_u N_{\text{UE}}^{(\text{FC})} T_{\text{target},u}^{(\text{FC})}$ 
  for each HUE do
     $N_{\text{PRB},u}^{(\text{FC})} \leftarrow \lceil \frac{T_{\text{target},u}^{(\text{FC})}}{T_{\text{target}}^{(\text{FC})}} \cdot (N_{\text{PRB}}^{(\text{FC})} - N_{\text{UE}}^{(\text{FC})} + 1) \rceil$ 
     $R \leftarrow \lceil g(\frac{T_{\text{target},u}^{(\text{FC})}}{N_{\text{PRB},u}^{(\text{FC})}}) \rceil$ 
    while  $Q < R$  &&  $P_{\text{Tx,CQI}}^{(\text{FC})} < P_{\text{Tx,max}}^{(\text{FC})}$  do
       $P_{\text{Tx,CQI}}^{(\text{FC})} = P_{\text{Tx,CQI}}^{(\text{FC})} + \Delta P_{\text{Tx}}$ 
    end while
  end for
end for

```

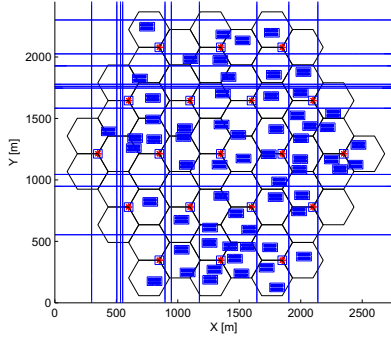


Fig. 3. Simulation environment, horizontal and vertical lines represent streets, “*”s are eNBs and rectangles are building blocks

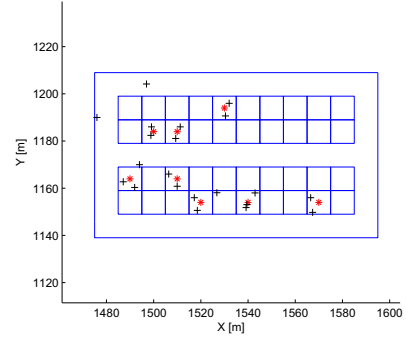


Fig. 4. Dual-stripe building model with red *’s as HeNBs and black +’s as UEs

the HeNB. Assuming the channel is flat, R can be obtained with a data rate to CQI mapping function $f(\cdot)$. $N_{\text{PRB},u}^{(\text{FC})}$ is calculated in the way that guarantees one HUE can get at least one PRB.

Assuming the interferences stay the same, to increase the CQI by 1, the increment of signal power $\Delta P_{\text{Tx},\text{CQI}}$ can be calculated with the inverse SNR to CQI mapping function, described in Fig. 2 (b). Moreover, several femtocells could have overlapped area, thus tuning one HeNB would affect the others. Considering this case, the increment used in this algorithm is set to $\Delta P_{\text{Tx}} = \Delta P_{\text{Tx},\text{CQI}}/2$.

The choice of α results in a trade-off between throughput and coverage. Larger α typically leads to larger average throughput but less coverage due to interference. Strictly speaking, the web user is rate adaptive, only if α approaches infinity. However, with a properly chosen α , desired throughput and coverage can be achieved. Furthermore, α can be configured by upper layer protocols, according to applications.

	HeNB	eNB
Carrier frequency	2 GHz	2GHz
Spectrum	1 MHz	10 MHz
Antenna pattern	Omni-directional	3-sector
Max. Tx power	20 dBm	46 dBm
Antenna gain	5 dBi	14 dBi

TABLE II
SIMULATION PARAMETERS.

eNB-indoor UE	$L_{m,u,\text{dB}}^{(\text{MC})} = 15.3 + 37.6 \log r_{m,u} + q \cdot L_{iw} + L_{ow}$
eNB-outdoor UE	$L_{m,v,\text{dB}}^{(\text{MC})} = 15.3 + 37.6 \log r_{m,v}$
HeNB-indoor UE	$L_{f,v,\text{dB}}^{(\text{FC})} = \max(38.46 + 20 \log r_{f,v}, 15.3 + 37.6 \log r_{f,v}) + 0.7d_{f,v} + q \cdot L_{iw}$
HeNB-outdoor UE	$L_{f,v,\text{dB}}^{(\text{FC})} = \max(38.46 + 20 \log r_{f,v}, 15.3 + 37.6 \log r_{f,v}) + 0.7d_{f,v} + q \cdot L_{iw} + L_{ow}$

TABLE III
PATHLOSS MODELS.

IV. PERFORMANCE EVALUATION

A. Simulation setup

In the simulation, an urban area with 19 eNBs, each equipped with 3-sector antennas, is considered. The inter-site distance is 500 meters. Buildings are modeled as dual-stripe blocks, where one building consists 40 apartments [14] as shown in Fig. 4. HeNBs are deployed in 20% of the randomly chosen apartments, where each HeNB is placed at the center of the apartment. Indoor UEs move randomly with pedestrian speed. Outdoor UEs can only move along the streets, which are randomly laid across the map, from north to south or from east to west. Moreover, outdoor UEs are divided into high speed vehicular UEs and low speed pedestrian UEs. The number of MUEs is 400, and 80% of them are indoor. Moreover, for each HeNB, 2 HUEs are in the same apartment. The parameters for user mobility is shown in Tab. IV. Some of the parameters for both macro and femtocells are summarized in Tab. II, whereas the pathloss models are summarized in Tab. III, where r is the distance between basestation and UE, d is the distance between the UE and its projection on the building wall, q is the number of inner walls separating basestation and UE, $L_{iw} = 5\text{dB}$ is the inner wall penetration loss and $L_{ow} = 10\text{dB}$ is the outer wall penetration loss.

Two metrics are used for comparing different power control schemes, namely, coverage and throughput. The coverage is defined by the proportion of satisfied UE in a certain group of UE. A web UE is satisfied, when its minimum data rate requirement is met. The throughput is averaged for each UE over the whole simulation. For VoIP and data UE, their throughput is equal to their data rate demand, when they are served. And for web UE, the throughput is the maximum achievable data rate according to their channel conditions.

Five different cases are compared for evaluation: (a). All HeNBs are turned off, namely, the macro-only scenario, denoted as “Off”; (b). The distance-based power control, denoted as “Dist”; (c). The measurement-based power control, denoted as “Meas”; (d). The proposed CQI-based power control, denoted as “CQI”; (e). All HeNBs transmit with maximum Tx power, denoted as “Max”.

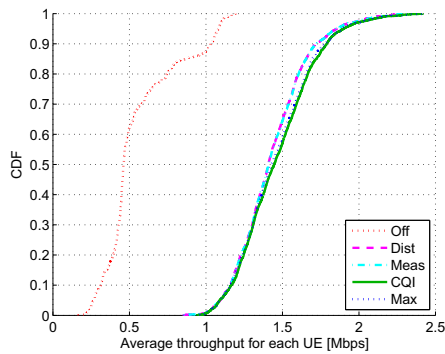


Fig. 5. Comparison of throughput of all UEs for different schemes, with $\alpha = 2$ Mbps

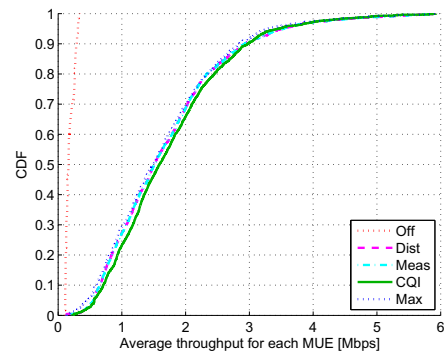


Fig. 7. Comparison of throughput of MUEs for different schemes, with $\alpha = 2$ Mbps

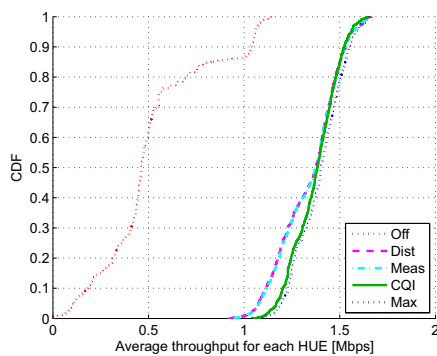


Fig. 6. Comparison of throughput of HUEs for different schemes, with $\alpha = 2$ Mbps

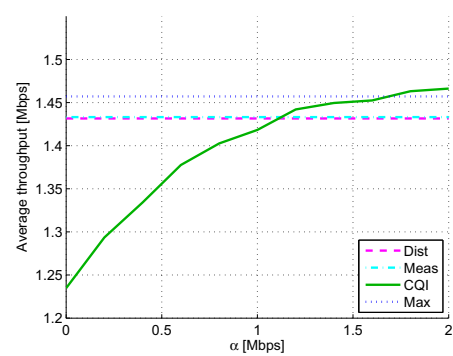


Fig. 8. Comparison of average throughput for different α

B. Simulation results

With α set to 2 Mbps, the average throughput of all UEs are compared in Fig. 5, which clearly shows, that a huge throughput gain can be obtained by using femtocells. The measurement-based power control and the distance-based power control perform almost the same. Transmitting with maximum power gives better throughput performance. The proposed CQI-based scheme offers the best throughput, because it has less interference to MUE comparing to maximum power and less interference to HUE of other femtocells in comparison of distance/measurement based schemes.

Using maximum Tx power, the throughput for HUEs is higher than using other schemes. This phenomena can be observed in Fig. 6. Moreover, the proposed CQI-based scheme also has better throughput than the distance/measurement-

User	Average speed	Mobility pattern
Outdoor pedestrian	1 m/s	Along streets
Outdoor vehicular	10 m/s	Along streets
Indoor pedestrian	1 m/s	Indoor, random

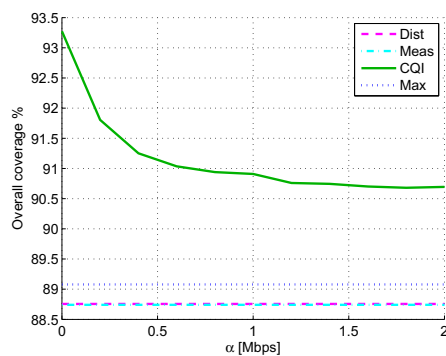
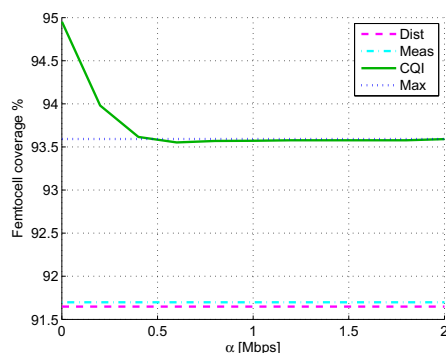
TABLE IV
USER MOBILITY PARAMETERS.

based schemes. The reason is, these two methods try to match the femtocell Rx power to the strongest macrocell Rx power. And for the femtocells located on the edge of macrocells, the macrocell Rx power is rather poor. For all HeNBs being turned off, the throughput is evaluated for the UEs which will be HUEs, if the HeNBs are switched on.

Comparing the MUE throughput, it is clear that using maximum Tx power causes large interference to the MUE, thus leads to a worse throughput, as can be seen in Fig. 7. In this figure, the CQI-based algorithm still shows the best performance, as a result of proper power management. And turning HeNBs off leads to a dramatic drop in throughput, due to the wall penetration loss.

As compared in Fig. 8, with small α , the average throughput of the CQI-based scheme is smaller than the distance/measurement based schemes, however, becomes larger with the increase of α . With $\alpha > 1.6$ the overall throughput of the CQI-based scheme is better than using maximum power, due to less interference to neighboring femtocells.

Regarding coverage, the overall user satisfaction rate is compared in Fig. 9, where the superiority of the proposed scheme is evident. Due to the trade-off between throughput and coverage [15], as α grows, coverage becomes worse. However, even after convergence, the proposed scheme can

Fig. 9. Comparison of overall coverage for different α Fig. 10. Comparison of femtocell coverage for different α

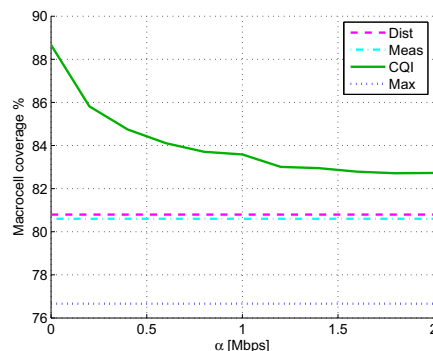
still provide more than 2% and 1.5% of coverage gain over the distance/measurement based algorithms and maximum Tx power, respectively.

The coverage for femtocells and macrocells are shown in Fig. 10 and Fig. 11, respectively. For femtocells, maximum Tx power has similar, sometimes even better performance, comparing to the proposed scheme, since the femtocells are unlikely to have overlapped coverage area. And because of the femtocells located on the edge of the macrocells, the distance/measurement based algorithms have rather poor femtocell coverage. The large Tx power of maximum power scheme results in poor coverage for macrocells. The distance/measurement based algorithms offer better macrocell coverage than maximum power, however, they still cannot compete with the proposed CQI-based scheme.

V. CONCLUSION

In this work, a decentralized CQI-based power control scheme is proposed for LTE femtocells. The proposed scheme does not make strong assumptions of the network, but only utilizes the channel feedback mechanism, which is already implemented in LTE. This property makes the proposed scheme easy to implement in a real system. An offset throughput is set for RA users to improve data rate. The network throughput

and coverage be balanced, by tuning the offset throughput.

Fig. 11. Comparison of macrocell coverage for different α

REFERENCES

- [1] H. Claussen, L. T. W. Ho, and L. G. Samuel, "Financial analysis of a pico-cellular home network deployment," in *Communications, IEEE International Conference on (ICC)*, Glasgow, Scotland, Jun. 2007.
- [2] E. Seidel and E. Saad, "LTE home node BS and its enhancements in release 9," Nomor Research White Paper, May 2010.
- [3] D. Calin, H. Claussen, and H. Uzunalioglu, "On femto deployment architectures and macrocell offloading benefits in joint macro-femto deployments," *Communication Magazine, IEEE*, vol. 48, no. 1, pp. 26–32, 2010.
- [4] H. Mahmoud and I. Guvenc, "A comparative study of different deployment modes for femtocell networks," in *Personal, Indoor and Mobile Radio Communications, IEEE 20th International Symposium on (PIMRC)*, Tokyo, Japan, Sep. 2009.
- [5] J. O'Carroll, H. Claussen, and L. Doyle, "Partial GSM spectrum reuse for femtocells," in *Personal, Indoor and Mobile Radio Communications, IEEE 20th International Symposium on (PIMRC)*, Tokyo, Japan, Sep. 2009.
- [6] M. Andrews, V. Capdevielle, A. Feki, and P. Gupta, "Autonomous spectrum sharing for mixed LTE femto and macro cells deployments," in *Computer Communications, IEEE Conference on (INFOCOM)*, San Diego, USA, Mar. 2010.
- [7] H. Claussen, L. T. W. Ho, and L. G. Samuel, "Self-optimization of coverage for femtocell deployments," in *Wireless Telecommunications Symposium, (WTS)*, Pomona, USA, Apr. 2008, pp. 278–285.
- [8] M. Morita, Y. Matsunaga, and K. Hamabe, "Adaptive power level setting of femtocell base stations for mitigating interference with macrocells," in *Vehicular Technology Conference Fall (VTC Fall), IEEE 72nd*, Ottawa, Canada, Sep. 2010.
- [9] 3GPP TS 36.213 V8.8.0, "Evolved universal terrestrial radio access (E-UTRA): Physical layer procedures," Sep. 2009.
- [10] X. Xu and R. Mathar, "Low complexity joint channel estimation and decoding for LDPC coded MIMO-OFDM systems," in *Vehicular Technology Conference (VTC Spring), IEEE 73rd*, Budapest, Hungary, May 2011.
- [11] K. E. Baddour and N. C. Beaulieu, "Autoregressive modeling for fading channel simulation," *Wireless Communications, IEEE Transactions on*, vol. 4, no. 4, pp. 1650–1662, Jul. 2005.
- [12] S. N. Donthi and N. B. Mehta, "An accurate model for EESM and its application to analysis of CQI feedback schemes and scheduling in LTE," *Wireless Communications, IEEE Transactions on*, vol. 10, no. 10, pp. 3436–3448, Oct. 2011.
- [13] C. Liu, A. Schmeink, and R. Mathar, "Dual optimal resource allocation for heterogeneous transmission in OFDMA systems," in *Globecom, IEEE*, Honolulu, Hawaii, USA, Dec. 2009.
- [14] 3GPP R4-092042, "Simulation assumptions and parameters for FDD HeNB RF requirements," Alcatel-Lucent, picoChip Designs, Vodafone.
- [15] A. Engels, M. Reyer, X. Xu, R. Mathar, J. Zhang, and H. Zhuang, "Autonomous self-optimization of coverage and capacity in LTE cellular networks," *IEEE Transactions on Vehicular Technology, Special Issue: Self-Organizing Radio Networks*, vol. 62, no. 5, pp. 1989–2004, 2013.